Journal of Ceramic Processing Research. Vol. 25, No. 5, pp. 790~797 (2024)
(Received 14 June 2024, Received in revised form 17 July 2024, Accepted 31 July 2024)
https://doi.org/10.36410/jcpr.2024.25.5.790

J O U R N A L O F
Ceramic Processing Research

Examining the impact of sintering conditions on the microwave dielectric properties of $Ca_{0.61}M_{0.26}TiO_3$ ($M=La^{3+}$, Nd^{3+})

Chun-Hsu Shen*, Chih-Hsuan Hu, Jing-Yuan Chen, Wen-Hui Chen, Chen-Wei Tung, Yun-Hsien Yang and Ting-Yu Yang
Department of Electronic Engineering, Ming Chuan University, 5 De Ming Rd., Gui Shan District, Taoyuan City 333, Taiwan

This research, which takes a unique approach, investigates the influence of calcination temperatures on the microwave dielectric properties of $Ca_{0.61}M_{0.26}TiO_3$ ($M=La^{3+}$, Nd^{3+}) ceramics. The samples were prepared using a conventional solid-state reaction method, with systematic variations in calcination temperatures. The sintering process, a crucial step in sample preparation, was conducted at a sintering temperature for a duration. The study focuses on critical dielectric parameters, such as dielectric constant (ε_r), quality factor (Qf values), and temperature coefficient (τ_f values), measured at microwave frequencies. The unique findings of this research highlight the importance of calcination temperatures in determining the ceramics' phase purity, grain size, and density, thereby influencing their dielectric properties. These original findings, not previously reported, identify optimal calcination temperatures for both $Ca_{0.61}La_{0.26}TiO_3$ and $Ca_{0.61}Nd_{0.26}TiO_3$, with each material exhibiting distinct temperature dependencies due to the different ionic radii and chemical properties of La^{3+} and Nd^{3+}. These original results significantly enhance our understanding of how calcination temperature affects microwave dielectric performance, offering essential guidance for developing high-performance dielectric materials for advanced communication technologies.

Keywords: Calcination temperature, Microwave, Dielectric properties, Dielectric materials.

Introduction

Microwave dielectric materials, which are crucial to modern communication technologies such as satellite communications, mobile phones, and GPS systems, must exhibit specific dielectric properties, such as a high dielectric constant (ε_r), low dielectric loss (high-quality factor, Qf), and a stable temperature coefficient of resonant frequency (τ_f) [1-7]. Among various ceramic materials, calcium titanate-based ceramics, particularly $Ca_{0.61}M_{0.26}TiO_3$ ($M=La^{3+}$, Nd^{3+}), have shown promise due to their favorable dielectric properties and thermal stability [8-13]. Therefore, this research has significant practical implications for developing high-performance dielectric materials. By understanding the effect of calcination temperature on the dielectric properties of these materials, researchers and engineers can optimize the manufacturing process, leading to the production of more efficient and reliable communication technologies. This makes it a crucial study for professionals in the field.

The synthesis process of these ceramics, especially the calcination stage, is crucial in determining their final dielectric properties. Calcination, a thermal treatment process, influences the precursor powders' phase formation, particle size, and homogeneity, subsequently affecting the microstructure and sintered ceramics' performance [14-19]. Previous studies have shown that calcination temperature significantly impacts ceramic materials' phase composition and densification behavior, ultimately affecting their dielectric properties. Despite the significance of calcination, there is a need for a systematic study to understand how different calcination temperatures impact the microwave dielectric properties of $Ca_{0.61}M_{0.26}TiO_3$ ($M=La^{3+}$, Nd^{3+}) ceramics.

This study aims to fill this gap by investigating the effects of varying calcination conditions (temperatures and holding times) on the microwave dielectric properties of $Ca_{0.61}Nd_{0.26}TiO_3$ and $Ca_{0.61}La_{0.26}TiO_3$. By examining these effects, the research seeks to optimize the calcination conditions to achieve superior dielectric performance. Understanding these relationships will provide valuable insights for the fabrication of high-performance microwave dielectric materials, contributing to advancements in communication technology.

Experimental Procedure

To investigate the impact of calcination temperature on the microwave dielectric properties of $Ca_{0.61}M_{0.26}TiO_3$ ($M=La^{3+}$, Nd^{3+}) ceramics, the following experimental procedure was employed:

*Corresponding author:
Tel : +886 3 350-7001 ext. 3737
Fax: +886 3 359-3877
E-mail: chshen0656@mail.mcu.edu.tw

Material Preparation

High-purity raw materials, such as $CaCO_3$, TiO_2, La_2O_3, and Nd_2O_3, were used as the initial powders. These powders were measured according to the stoichiometric ratio of $Ca_{0.61}M_{0.26}TiO_3$ (where M represents La^{3+} or Nd^{3+}). They were then combined and thoroughly homogenized using a planetary ball mill with agate balls for 24 hours, utilizing distilled water as the milling medium.

Calcination

The homogenized powder mixtures were first dried and then calcined. This process was carried out at different temperatures, specifically 1100 °C and 1200 °C, with withholding times ranging from 1 to 6 hours in the air, to investigate the impact of temperature. Following calcination, the powders were ground to break up any agglomerates that had formed during the thermal treatment.

Sintering

The calcined powders were compressed into cylindrical pellets utilizing a uniaxial press at a pressure of 200 MPa. These pellets underwent sintering in air at temperatures ranging from 1350 °C to 1450 °C for durations spanning 1 to 5 hours. These sintering conditions were established through prior experimentation to achieve optimal densification.

Characterization

X-ray diffraction (XRD) was employed to analyze the phase composition of both the calcined and sintered samples, ensuring phase purity and detecting any secondary phases. Additionally, scanning electron microscopy (SEM) was utilized to investigate the microstructure and particle size of the sintered samples. The bulk density of these sintered samples was determined through the Archimedes method.

Microwave Dielectric Property Measurements

The dielectric constant (ε_r) and quality factor (Qf) were determined using a network analyzer operating within microwave frequency ranges. For the assessment of the temperature coefficient of resonant frequency (τ_f), measurements were conducted by tracking the resonant frequency over a temperature range spanning from 25 °C to 85 °C [20, 21].

Data Analysis

The influence of calcination temperature on dielectric properties was investigated by contrasting the ε_r, Qf, and τ_f values of samples subjected to varying calcination temperatures and durations. These findings were then correlated with the samples' phase composition, microstructure, and density to pinpoint the optimal calcination temperature for each composition $Ca_{0.61}M_{0.26}TiO_3$ ($M=La^{3+}$, Nd^{3+}).

Results and Discussion

X-ray diffraction (XRD) analysis was conducted to examine the phase composition and crystallographic structure of $Ca_{0.61}M_{0.26}TiO_3$ ($M=La^{3+}$, Nd^{3+}) ceramics

Table 1. XRD results of $Ca_{0.61}M_{0.26}TiO_3$ ($M = La^{3+}$, Nd^{3+}) ceramics at different calcine temperatures and holding times (top 4 intensities).

$CaTiO_3$				
1100°C/1hr	63840	42143	19033	10641
1100°C/2hr	73943	40657	20034	9096
1100°C/3hr	72834	35822	17788	9713
1100°C/4hr	**77842**	**44302**	**20863**	**10368**
1100°C/5hr	66639	42816	19046	11087
1100°C/6hr	79631	37906	19940	10630
1200°C/1hr	77873	39590	17422	11571
1200°C/2hr	76568	40036	18832	10980
1200°C/3hr	63022	39273	17381	10268
1200°C/4hr	80444	41561	20256	9723
1200°C/5hr	74124	38695	19157	9561
1200°C/6hr	70549	43945	19858	10430
$Ca_{0.61}La_{0.26}TiO_3$				
1100°C/1hr	24672	11346	6030	3806
1100°C/2hr	30175	11670	6989	4049
1100°C/3hr	29617	11752	7436	4023
1100°C/4hr	32199	11798	8003	3938
1100°C/5hr	33870	12003	8435	4491
1100°C/6hr	34674	11869	8231	3879
1200°C/1hr	38385	13969	10981	5078
1200°C/2hr	47116	16626	12848	5310
1200°C/3hr	**56224**	**20743**	**15697**	**6963**
1200°C/4hr	44159	16891	12537	5367
1200°C/5hr	54407	18900	14400	6516
1200°C/6hr	29242	12082	9400	4129
$Ca_{0.61}Nd_{0.26}TiO_3$				
1100°C/1hr	50817	22128	13902	5689
1100°C/2hr	58959	23034	15440	6444
1100°C/3hr	65944	25023	16592	6540
1100°C/4hr	66643	29654	17602	7898
1100°C/5hr	49732	22701	14716	7000
1100°C/6hr	69172	28515	17577	7505
1200°C/1hr	**70412**	**27912**	**17384**	**7417**
1200°C/2hr	46057	21634	12906	5699
1200°C/3hr	22753	12399	8694	4428
1200°C/4hr	46365	20634	13164	6489
1200°C/5hr	39942	17459	11614	5691
1200°C/6hr	29370	13675	9604	5026

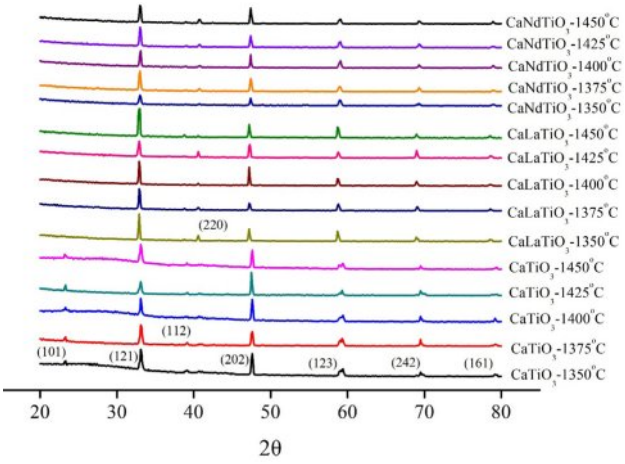

Fig. 1. The XRD results of $Ca_{0.61}M_{0.26}TiO_3$ (M=La^{3+}, Nd^{3+}) ceramics at different sintering temperatures.

calcined at various temperatures and holding times are shown in Table 1. Upon comparing with JCPDS (42-0423), we confirmed that all samples are perovskite compositions. We compared the four most substantial peaks and proceeded with the experimental step. The calcination conditions chosen are 1200 °C for 3 hours for $Ca_{0.61}La_{0.26}TiO_3$ and 1200 °C for 1 hour for $Ca_{0.61}Nd_{0.26}TiO_3$. Fig. 1 displays the XRD diffraction patterns of $Ca_{0.61}M_{0.26}TiO_3$ (M=La^{3+}, Nd^{3+}) ceramics sintered at different temperatures (1350 °C to 1450 °C) for 4 hours. Fig. 2 shows the diffraction patterns of these ceramics sintered at their optimal temperatures for varying holding times. As depicted in the figure, all results exhibit a single perovskite structure, indicating that changes in calcination temperature have minimal effect on the composition of the crystalline phase.

Table 1 illustrates the lattice constants of $Ca_{0.61}M_{0.26}TiO_3$ (M=La^{3+}, Nd^{3+}) ceramics after sintering for 4 hours at

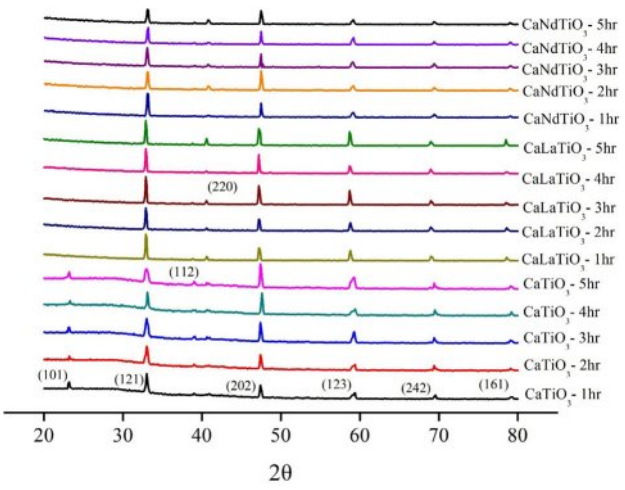

Fig. 2. The XRD results of $Ca_{0.61}M_{0.26}TiO_3$ (M=La^{3+}, Nd^{3+}) ceramics at their optimum sintering temperatures for various holding times.

Table 2. The lattice parameters of $Ca_{0.61}M_{0.26}TiO_3$ (M = La^{3+}, Nd^{3+}) ceramics sintered at varied temperatures for four h.

$CaTiO_3$			
S.T.(°C)	a(Å)	b(Å)	c(Å)
1350	5.4467±0.0120	7.6406±0.0091	5.3783±0.0059
1375	5.4339±0.0119	7.6406±0.0091	5.3906±0.0060
1400	5.4467±0.0120	7.6406±0.0091	5.3783±0.0059
1425	5.4143±0.0065	7.6515±0.0050	5.3885±0.0033
1450	5.4510±0.0004	7.6316±0.0003	5.3737±0.0002
$Ca_{0.61}La_{0.26}TiO_3$			
S.T.(°C)	a(Å)	b(Å)	c(Å)
1350	5.4599±0.0069	7.7469±0.0181	5.5517±0.0460
1375	5.4330±0.0010	7.6961±0.0026	5.4465±0.0064
1400	5.4522±0.0029	7.7263±0.0077	5.5232±0.0193
1425	5.4211±0.0040	7.6343±0.0103	5.3505±0.0244
1450	5.4445±0.0129	7.7062±0.0335	5.4959±0.0835
$Ca_{0.61}Nd_{0.26}TiO_3$			
S.T.(°C)	a(Å)	b(Å)	c(Å)
1350	5.4162±0.0023	7.6627±0.0038	5.4180±0.0062
1375	5.4162±0.0023	7.6627±0.0038	5.4180±0.0062
1400	5.4132±0.0040	7.6630±0.0046	5.4457±0.0077
1425	5.4037±0.0033	7.6627±0.0038	5.4306±0.0063
1450	5.3953±0.0127	7.6561±0.0148	5.4214±0.0242

(S.T.: Sintering Temperature)

different temperatures, and Table 2 displays the lattice constants of $Ca_{0.61}M_{0.26}TiO_3$ (M=La^{3+}, Nd^{3+}) ceramics sintered at 1400 °C for varying holding times. Typically, the effects of elemental substitution on the lattice constant encompass considerations such as ionic radius, valence, crystal structure, and other relevant factors. Based on the findings, the lattice constant remains relatively unchanged after substituting La^{3+} and Nd^{3+}. This indicates that the ionic radii of La^{3+} (1.22 Å) and Nd^{3+} (1.15 Å) may not differ significantly from that of Ca^{2+} (1.06 Å) and that the chemical formula has attained a valence equilibrium. Additionally, the XRD analysis confirms the continued presence of the perovskite structure of $CaTiO_3$, indicating no observable alteration resulting from the substitution of La^{3+} and Nd^{3+}.

The utilization of scanning electron microscopy (SEM) offers valuable insights into the microstructural characteristics of $Ca_{0.61}M_{0.26}TiO_3$ (M=La^{3+}, Nd^{3+}) ceramics are shown in Fig. 3 (for $CaTiO_3$) and Fig. 4 ($Ca_{0.61}La_{0.26}TiO_3$ and $Ca_{0.61}Nd_{0.26}TiO_3$). The particle size variation with sintering temperature can be observed through SEM analysis of $Ca_{0.61}M_{0.26}TiO_3$ (M=La^{3+}, Nd^{3+}) ceramics. Generally, at lower sintering temperatures, as shown in Fig. 3(a), Fig. 4(a), and (f), the particles tend to be smaller and more dispersed due to insufficient energy for grain growth and consolidation. As the sintering temperature increases, as shown in Fig. 3(c), Fig. 4(c),

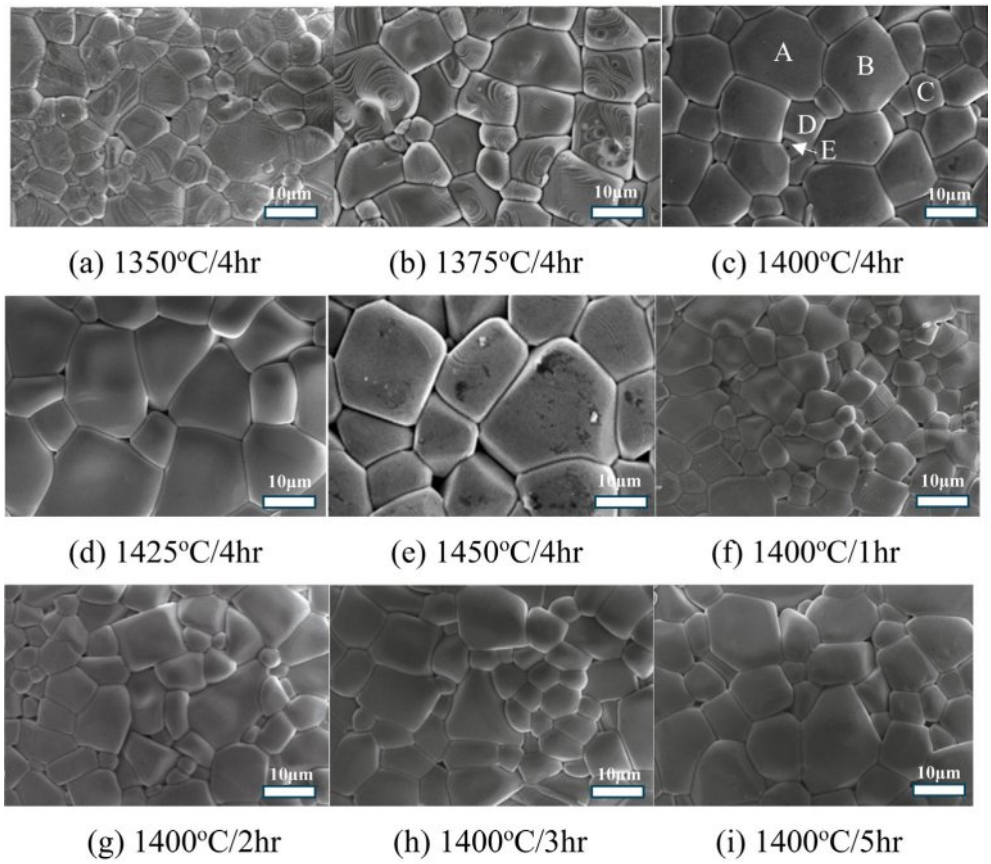

Fig. 3. The SEM images of $CaTiO_3$ ceramics were obtained with various sintering temperatures and holding times.

and (h), the energy available for atomic diffusion and grain boundary migration also increases, promoting particle growth. An optimal balance between particle growth and densification is achieved at intermediate sintering temperatures, resulting in well-defined grain boundaries and a uniform particle size distribution. This is often associated with enhanced mechanical properties and improved electrical conductivity. However, at excessively high sintering temperatures, as shown in Fig. 3(e), Fig. 4(e), and (j), particle coarsening may occur, leading to the formation of large particles and possible grain boundary discontinuities. This can adversely affect the material's properties by increasing its susceptibility to mechanical failure and reducing its electrical performance [22-26]. In summary, SEM analysis of $Ca_{0.61}M_{0.26}TiO_3$ ($M=La^{3+}$, Nd^{3+}) ceramics reveals that particle size tends to increase with sintering temperature up to an optimum, beyond which further increases may lead to detrimental effects on microstructural homogeneity and material properties. Comparable outcomes may arise concerning the holding time at a particular temperature, shown in Fig. 3(f)-(i), wherein particle size augmentation is observable until an optimal threshold is reached. Beyond this point, a continued increase in particle size could detrimentally impact microstructural consistency and material characteristics.

The Energy Dispersive X-ray Spectroscopy (EDS) analysis results provide valuable information regarding the elemental composition of $Ca_{0.61}M_{0.26}TiO_3$ ($M=La^{3+}$, Nd^{3+}) ceramics are shown in Table 4. The EDS analysis reveals the elemental composition of the ceramic, including the concentrations of calcium (Ca), titanium (Ti), and the substituent elements La and Nd. The EDS findings indicate that, regardless of their visual characteristics, the grains predominantly consist of $Ca_{0.61}M_{0.26}TiO_3$ ($M=La^{3+}$, Nd^{3+}), a conclusion that aligns with the XRD analysis results discussed earlier.

The relationship between density and dielectric constant (ε_r) with sintering temperature can be elucidated through experimental observations of $Ca_{0.61}M_{0.26}TiO_3$ ($M=La^{3+}$, Nd^{3+}) ceramics are shown in Fig. 5. Generally, as the sintering temperature increases, the density of the ceramics tends to rise due to enhanced particle rearrangement and densification processes. This increase in density is often accompanied by a corresponding improvement in the dielectric constant (ε_r) of the ceramics, as a denser microstructure allows for more efficient polarization of the material under an applied electric field. At lower sintering temperatures, where densification is incomplete, the ceramics may exhibit lower densities and dielectric constants (ε_r) due to voids, pores, and incomplete particle bonding. As the sintering temperature is raised to an optimal range, densification becomes more complete, resulting in higher densities and

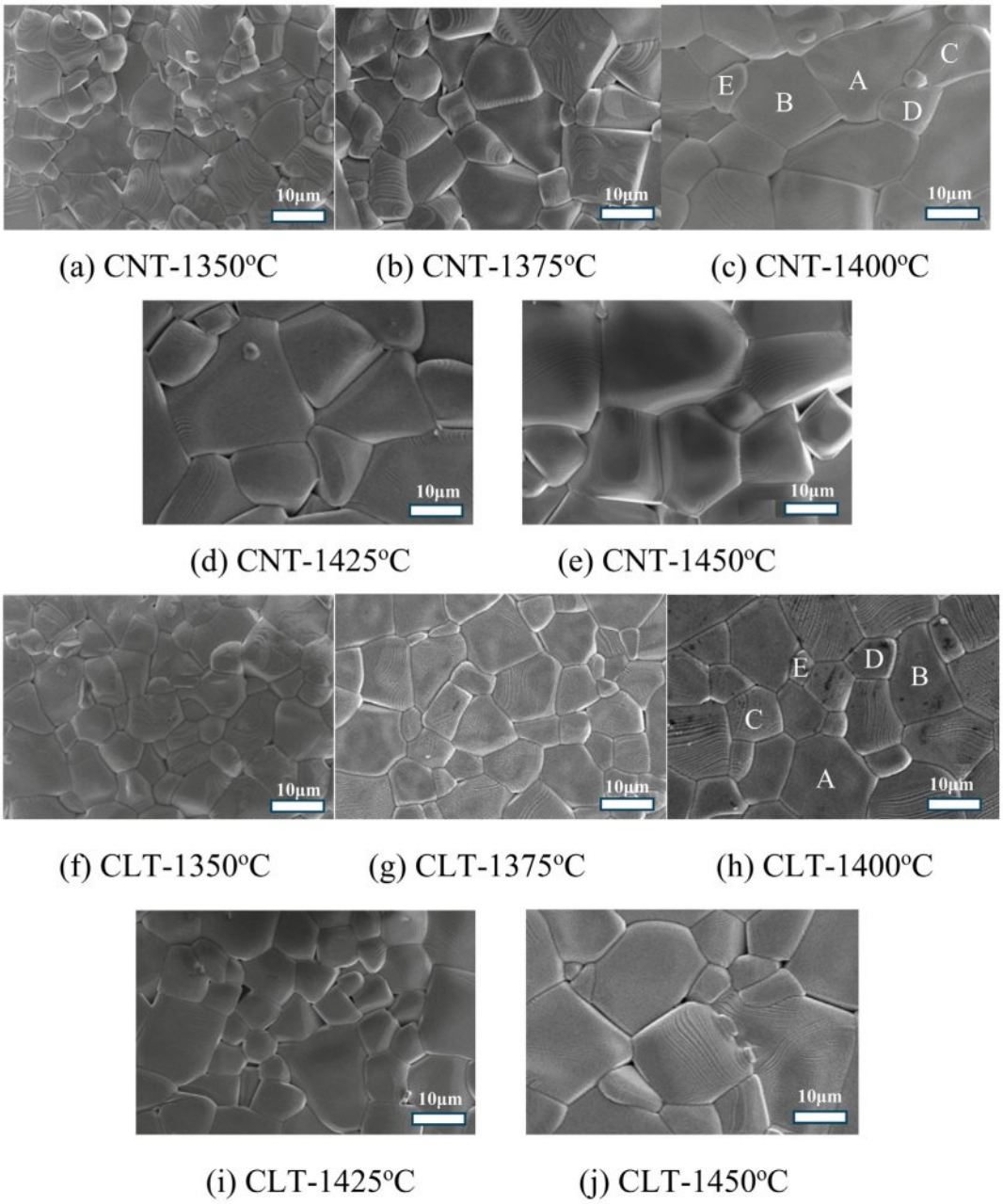

Fig. 4. The SEM images of $Ca_{0.61}M_{0.26}TiO_3$ ($M=La^{3+}$, Nd^{3+}) ceramics were obtained with various sintering temperature for 4hr.

improved dielectric properties. However, over-sintering may occur at excessively high sintering temperatures, leading to grain coarsening and the formation of voids or defects. This can result in a decrease in density and, consequently, a reduction in the dielectric constants (ε_r) of the ceramics. Additionally, excessive grain growth may disrupt the uniformity of the microstructure, leading to variations in dielectric properties across the material. In summary, the density and dielectric constant (ε_r) of $Ca_{0.61}M_{0.26}TiO_3$ ($M=La^{3+}$, Nd^{3+}) ceramics generally increase with sintering temperature up to an optimal range, beyond which further increases may lead to diminishing returns or even deterioration in material properties due to over-sintering effects.

The variation of quality factor (*Qf* values) with sintering temperature can be observed through experimental measurements of $Ca_{0.61}M_{0.26}TiO_3$ ($M=La^{3+}$, Nd^{3+}) ceramics are illustrated in Fig. 6. The quality factor, often denoted as Q, measures the energy losses in a resonant system, such as a capacitor or an inductor, relative to the stored energy. Typically, the *Qf* values of ceramics exhibit a non-linear relationship with sintering temperature. At lower sintering temperatures, where densification is incomplete, the material may contain defects, voids, or grain boundaries that contribute to energy losses and reduce the *Qf* values [27-30]. As the sintering temperature increases, densification improves, resulting in fewer defects and a more homogeneous

Table 3. The lattice parameters of $Ca_{0.61}M_{0.26}TiO_3$ (M = La^{3+}, Nd^{3+}) ceramics sintered at 1400 ºC for varied holding times.

$CaTiO_3$			
H.T.(hr)	a(Å)	b(Å)	c(Å)
1	5.4388±0.0243	7.6049±0.0144	5.3648±0.0125
2	5.4589±0.0124	7.6433±0.0074	5.3661±0.0063
3	5.4460±0.0123	7.6433±0.0074	5.3784±0.0064
4	5.4207±0.0053	7.6547±0.0032	5.3750±0.0027
5	5.4460±0.0123	7.6433±0.0074	5.3784±0.0064
$Ca_{0.61}La_{0.26}TiO_3$			
H.T.(hr)	a(Å)	b(Å)	c(Å)
1	5.4335±0.0007	7.6903±0.0008	5.4505±0.0013
2	5.4292±0.0075	7.6869±0.0086	5.4458±0.0141
3	5.4505±0.0089	7.6936±0.0102	5.4425±0.0166
4	5.4292±0.0320	7.6770±0.0365	5.4198±0.0594
5	5.4462±0.0007	7.6903±0.0008	5.4378±0.0013
$Ca_{0.61}Nd_{0.26}TiO_3$			
H.T.(hr)	a(Å)	b(Å)	c(Å)
1	5.4066±0.0114	7.6638±0.0132	5.4339±0.0217
2	5.3939±0.0126	7.6539±0.0146	5.4200±0.0239
3	5.4022±0.0207	7.6507±0.0239	5.4030±0.0388
4	5.4117±0.0039	7.6607±0.0045	5.4442±0.0075
5	5.3939±0.0126	7.6539±0.0146	5.4200±0.0239

H.T.: Holding Time

Table 4. The EDS results of particle formation for various spots are in Figure 3 (c), 4(c), and 4(h).

3(c) - **$CaTiO_3$**					
	Atom (%)				
Spot	Ca	La	Nd	Ti	O
A	21.84	0	0	18.78	59.38
B	22.82	0	0	19.77	57.41
C	21.56	0	0	18.29	60.15
D	23.28	0	0	20.39	56.33
E	21.49	0	0	18.85	59.66
4(c) - **$Ca_{0.61}Nd_{0.26}TiO_3$**					
	Atom (%)				
Spot	Ca	La	Nd	Ti	O
A	10.26	0	4.37	16.83	68.53
B	10.54	0	4.49	17.28	67.68
C	11.35	0	4.84	18.61	65.20
D	11.83	0	5.04	19.39	63.74
E	8.64	0	3.68	14.17	73.51
4(h) - **$Ca_{0.61}La_{0.26}TiO_3$**					
	Atom (%)				
Spot	Ca	La	Nd	Ti	O
A	10.77	4.91	0	18.79	65.53
B	12.23	5.91	0	21.57	60.28
C	11.35	4.89	0	18.57	65.20
D	12.22	5.28	0	19.76	62.74
E	8.54	3.97	0	14.98	72.51

microstructure. This can lead to a gradual increase in the *Qf* values of the ceramics. However, over-sintering may occur at excessively high sintering temperatures, causing grain coarsening and forming defects or grain boundary phases that can degrade the material's performance. This can decrease the *Qf* values as energy losses increase due to the presence of these detrimental features. In summary, the *Qf* values of $Ca_{0.61}M_{0.26}TiO_3$ ceramics typically increase with sintering temperature as densification improves, followed by a possible decline at excessively high temperatures due to over-sintering effects. When sintering at 1400 °C/4 h, the highest *Qf* value is 19,400 (GHz) for $Ca_{0.61}La_{0.26}TiO_3$, 18,600 (GHz) for $Ca_{0.61}Nd_{0.26}TiO_3$. Optimizing the sintering temperature is crucial to achieving the highest quality factor and maximizing the performance of the ceramic

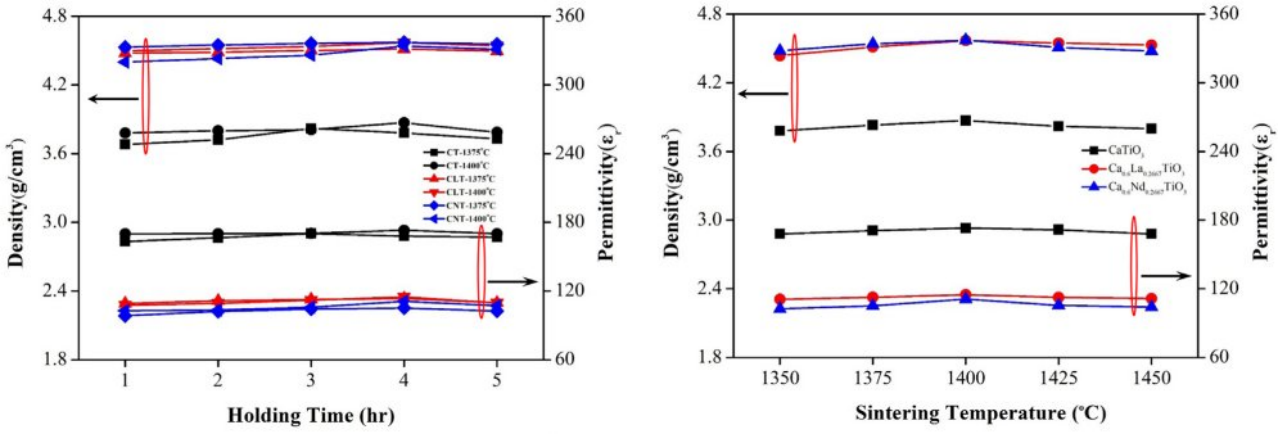

Fig. 5. The apparent density (D) and dielectric constant (ε_r values) of $Ca_{0.61}M_{0.26}TiO_3$ ($M=La^{3+}$, Nd^{3+}) ceramics with various holding times and sintering at varied temperatures.

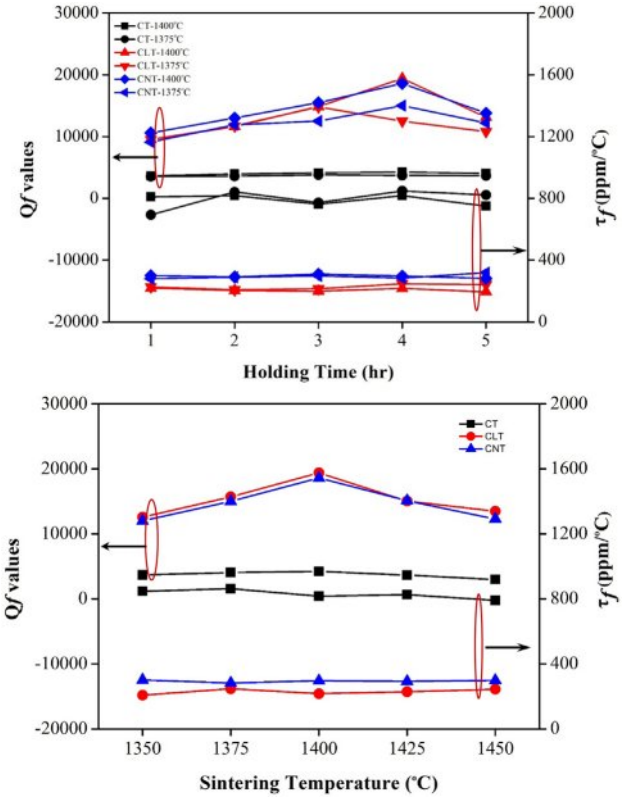

Fig. 6. Qf and τ_f values of $Ca_{0.61}M_{0.26}TiO_3$ (M=La^{3+}, Nd^{3+}) ceramics with various holding times and sintering at varied temperatures.

material in various applications.

The temperature coefficient (τ_f values) primarily investigates the susceptibility of materials' dielectric properties to ambient temperature changes. Generally, the τ_f values are predominantly influenced by the composition and presence of secondary phases within the material mixture. As can be seen from Fig. 6, the τ_f values do not change with the sintering temperature or holding times.

In summary, modifying the calcination conditions has improved the dielectric properties of $Ca_{0.61}M_{0.26}TiO_3$

Table 5. The dielectric performances of $Ca_{0.61}M_{0.26}TiO_3$ (M = La^{3+}, Nd^{3+}) ceramics with various calcine temperatures and sintering at their optimal temperature.

$Ca_{0.6}La_{0.267}TiO_3$				
	C.T.	ε_r	Qf(GHZ)	τ_f(ppm/°C)
[9]	1100 °C/4hr	109	17,600	+213
This work	1200 °C/3hr	114.8	19,400	+216.6
Comparison		+5.32%	+10.22%	+1.7%
$Ca_{0.6}Nd_{0267}TiO_3$				
	C.T.	ε_r	Qf(GHZ)	τ_f(ppm/°C)
[8]	1100 °C/4hr	108	17,000	+270
This work	1200 °C/3hr	110.9	18,600	+296.1
Comparison		+2.69%	+9.41%	+9.66%

Table 6. The dielectric performances with various x values for (1-x) $MgTiO_3$-x$Ca_{0.6}La_{0.8/3}TiO_3$ ceramics.

x values	S.T. (°C)	D (g/cm^3)	ε_r	Qf (GHZ)	τ_f (ppm/°C)
0.05	1400	3.73	18.2	131,900	–27.8
0.10		3.89	22	115,300	–11.9
0.15		3.97	25.8	108,000	–0.8
0.20		3.96	27	72,500	–11

(M=La^{3+}, Nd^{3+}) ceramics. The corresponding dielectric properties are summarized in Table 5. To delve deeper into the enhancing use temperature characteristics, we blended $Ca_{0.61}La_{0.26}TiO_3$ and $MgTiO_3$ to mitigate the temperature-related variations. The corresponding dielectric properties are detailed in Table 6. The data from Table 6 illustrates that incorporating $Ca_{0.61}La_{0.26}TiO_3$ enhances the temperature characteristics of $MgTiO_3$. This implies that by appropriately adjusting the content of $Ca_{0.61}La_{0.26}TiO_3$, the material composition can achieve superior temperature stability. Overall, the refinement of temperature characteristics in dielectric materials is vital for ensuring electronic components' reliability and optimal performance across varying thermal environments.

Conclusion

Through experimental verification, we have confirmed that modifying the calcination conditions of the material can positively influence the dielectric properties of the $Ca_{0.61}M_{0.26}TiO_3$ (M=La^{3+}, Nd^{3+}) ceramics. Adjusting the calcination temperature increased the quality factor (Qf values) by 10% in $Ca_{0.61}La_{0.26}TiO_3$ and 9% in $Ca_{0.61}Nd_{0.26}TiO_3$. To evaluate the effect on temperature characteristics, we experimented with mixing $Ca_{0.61}La_{0.26}TiO_3$ and $MgTiO_3$ into a dielectric ceramic system. The results show significant improvements in temperature stability. Highly temperature-stable dielectric material composition can be achieved by appropriately adjusting the ratio of $Ca_{0.61}La_{0.26}TiO_3$ to $MgTiO_3$. When the ratio of $Ca_{0.61}La_{0.26}TiO_3$ to $MgTiO_3$ is 85:15, the dielectric characteristics obtained are a dielectric constant (ε_r) of 25.8, a Qf value of 108,000 (GHz), and a temperature coefficient (τ_f) of -0.8 (ppm/°C).

References

1. P.C. Chen, C.L. Pan, K.C. Lin, and C.H. Shen, J. Ceram. Process. Res. 25[2] (2024) 278-284.
2. Y.S. Park and E.S. Kim, J. Ceram. Process. Res. 23[6] (2022) 920-926.
3. S. Kim, J. Ceram. Process. Res. 18[6] (2017) 421-424.
4. M.C. Paul, A. Dhar, S. Das, M. Pal, S.K. Bhadra, A.M. Markom, N.S. Rosli, A. Hamzah, H. Ahmad, and S.W. Harun, IEEE Photonics J. 7[5] (2015).
5. Y. Jang, J. Kim, S. Kim, and K. Lee, IEEE Microw. Wirel. Common. Lett. 24 (2014) 665-667.

6. K. Wakino, K. Minal, and H. Tamura, J. Am. Ceram. Soc. 67[4] (1984) 278-281.
7. S. Nomura, K. Toyama, and K. Kaneta, Jpn. J. Appl. Phys. 21 (1982) L624-L626.
8. M. Yoshida, N. Hara, T. Takada, and A. Seki, Jpn. J. Appl. Phys. 36 (1997) 6818-6823.
9. C.L. Huang, J.T. Tasi, and Y.B. Chen, Mater. Res. Bull. 36[3-4] (2001) 547-556.
10. C.L. Huang, C.F. Tasi, and Y.B. Chen, J. Alloy Comp. 453[1-2] (2008) 337-340.
11. C.L. Huang, Y.B. Chen, and C.F. Tasi, J. Alloy Comp. 454[1-2] (2008) 454-459.
12. V. M. Ferreira, F. Azough, J.L. Baptista, and R. Freer, J. Mater. Res. 12[12] (1992) 3293-3299.
13. I.S. Kim, W.H. Jung, Y. Inaguma, and T. Nakamura, Mater. Res. Bull. 30[3] (1995) 307-316.
14. X. Kuang, G. Carotenuto, and L. Nicolais, Adv. Perform. Mater. 4 (1997) 257-274.
15. N. Saikumari, S. Monish Dev, and S. Avinaash Dev, Sci. Rep. 11 (2021) 1734-1751.
16. Y. Fang, A. Hu, S. Ouyang, and J.J. Oh, J. Eur. Ceram. Soc. 21 (2001) 2745-2750.
17. Y.F. Chen, C.Y. Lee, M.Y. Yeng, and H.T. Chiu, J. Cryst. Growth 247 (2003) 363-370.
18. Y.J. Choi, J.H. Park, J.H. Park, S. Nahm, and J.G. Park, J. Eur. Ceram. 27[4] (2007) 2017-2024.
19. T. Bongkarn and C. Wattanawikkam, Ferroelectrics 382 (2009) 42-48.
20. B.W. Hakki and P.D. Coleman, IRE Trans. Microwave Theory Tech. 8 (1960) 402-410.
21. W.E. Courtney, IEEE Trans. Microwave Theory Tech. 18 (1970) 476-485.
22. C.H. Shen and C.L. Pan, Int. J. Appl. Ceram. Technol. 12 (2015) E127-E133.
23. C.L. Huang and J.Y. Chen, J. Alloy. Compd. 485 (2009) 706-710.
24. C.L. Huang, S.S. Liu, and S.H. Chen, Jpn. J. Appl. Phys. 48 (2009) 071402-071404.
25. C.L. Huang and S.S. Liu, J. Alloy. Compd. 471 (2009) L9-L12.
26. C.L. Huang, J.J. Wang, and Y.P. Chang, J. Am. Ceram. Soc. 90 (2007) 858-862.
27. B.D. Silverman, Phys. Rev. 125 (1962) 1921-1928.
28. G.L. Gurevich and A.K. Tagantsev, Sov. Phys. JETP. 64 (1986) 142-151.
29. V.L. Gurevich and A.K. Tagantsev, Adv. Phys. 40 (1991) 719-767.
30. D. Kajfezz and P. Guillon, "Dielectric Resonators," (Noble Publishing Corporation, Atlanta, US 1998).